Journal of Environmental Science, Health & Sustainability, 2026, 2(1), 30–50
https://journals.enviromindsolutions.com/jeshs
eISSN: 3067-946X

Article

Critical Zone weathering controls on the hydrogeochemistry and spatial variability of groundwater arsenic and fluoride in the Lake Victoria Basin, Northwest Tanzania

Fanuel Ligate[1,2,3*], Julian Ijumulana[1,2], Regina Irunde[1,2], Vivian Kimambo[1,2], Rajabu Hamisi[1], Jyoti Prakash Maity[4,5], Joseph Mtamba[2], Felix Mtalo[2] and Prosun Bhattacharya[1,6]

[1]KTH-International Groundwater Arsenic Research Group, Department of Sustainable Development, Environmental Science and Engineering, KTH Royal Institute of Technology, SE-11428 Stockholm, Sweden
[2]DAFWAT Research Group, Department of Water Resources Engineering, College of Engineering and Technology, University of Dar es Salaam, Dar es Salaam, Tanzania
[3]Department of Chemistry, Mkwawa University College of Education, University of Dar es Salaam, 2513 Iringa, Tanzania
[4]Department of Chemistry, School of Applied Sciences, KIIT Deemed to be University, Bhubaneswar, Odisha 751024, India
[5]Centre for Water Research and Climate Change (CWRCC), under Centers for Innovations & Research (COIR), KIIT Deemed to be University, Bhubaneswar, Odisha 751024, India
[6]Centre for Research in Environment, Sustainability Advocacy and Climate Change, Directorate of Research, SRM Institute of Science and Technology, Kattankulathur - 603203, Tamil Nadu, India

How to cite

Ligate, F., Ijumulana, J., Irunde, R., Kimambo,V., Hamisi, R., Maity, J.P., Mtamba, J., Mtalo, F., Bhattacharya, P., 2026. Critical Zone weathering controls on the hydrogeochemistry and spatial variability of groundwater arsenic and fluoride in the Lake Victoria Basin, Northwest Tanzania. Journal of Environmental Science, Health & Sustainability, 2(1), 30–50.
https://doi.org/10.63697/jeshs.2026.10033

Article info

Received: 28 May 2025
Revised: 10 November 2025
Accepted: 15 November 2025
Published: 1 February 2026

Keywords

Critical Zone process
Arsenic and fluoride
Hydrogeochemistry
Geospatial analysis
Lake Victoria Basin

Graphical abstract

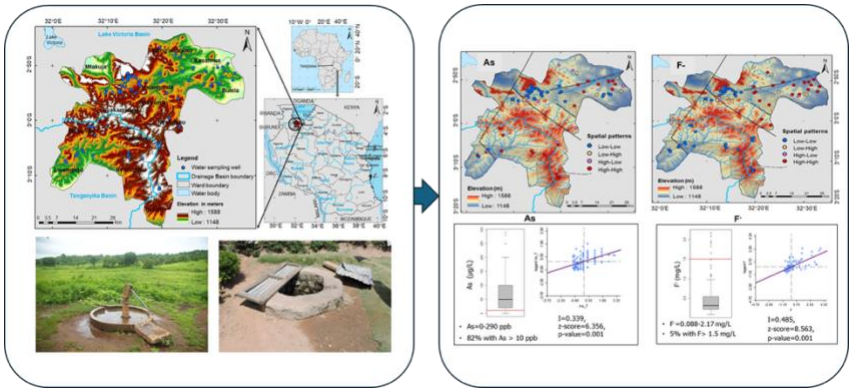

Highlights

- *As and F^- co-occurrence in groundwater in the Lake Victoria Basin region was studied.*
- *As concentrations exceeding the WHO guideline values in 82% of the groundwater samples.*
- *Eight percent of groundwater samples contained F^- concentrations exceeding the WHO guideline values.*
- *Critical Zone weathering is an important mechanism of mobilization of As, F^-, and other trace elements from geogenic sources.*

Abstract

Arsenic (As) and fluoride (F^-) in groundwater limit access to safe drinking water across East Africa, yet process-based understanding of their co-occurrence in Precambrian basement aquifers of northern Tanzania remains limited. This study analyzed groundwater samples (*n* = 88) from 13 wards in Geita district, Lake Victoria Basin, adjacent to large-scale and

*Corresponding author: fanuel.ligate@udsm.ac.tz (FL)
© 2026 The Authors. Published by Enviro Mind Solutions.
Handling Editor: Dr. Bibhash Nath with assistance from Dr.Abida Farooqi.

artisanal gold mining areas. An integrated approach combining hydrogeochemistry, geospatial analysis, and geochemical modeling was used to investigate spatial variability and the hydrogeochemical processes controlling the distribution of As and F^- in the aquifer. Arsenic concentrations ranged from 2.5 to 280 µg/L and F^- from 0.13 to 2.17 mg/L; with approximately 82% and 8% samples exceeding World Health Organization (WHO) guideline values, respectively. Groundwater pH was 5.7–7.5, electrical conductivity (EC) and total dissolved solids (TDS) indicated generally acceptable salinity and dissolved As occurred predominantly as As(V) species. As and F^- exhibited spatial clustering and co-occurrence associated with migmatite-granitoid-metasediment complexes and volcano-sedimentary Greenstone Belt lithologies, with higher concentrations observed in mining-affected areas. These patterns are interpreted within a Critical Zone framework, where coupled lithological, hydrological, and biogeochemical processes regulate weathering reactions, generate reactive Fe-oxide and clay surfaces, and establish pH and redox conditions that control trace element mobility. Variations in pH (5.7–7.5) influenced As mobility primarily through oxidative weathering of arsenopyrite and other sulfides, forming secondary Fe(III) oxides and hydroxides. Subsequent reductive dissolution of these Fe phases under favorable geochemical conditions released sorbed or co-precipitated As into groundwater, particularly within Ca-HCO_3 type waters. Fluoride mobilization was enhanced under alkaline, Na–HCO_3 waters, low Ca^{2+} activity, elevated Na^+ and HCO_3^-, ion exchange, and calcite precipitation, which together favored fluorite dissolution and desorption. By linking observed spatial patterns to Critical Zone weathering processes, this study provided a mechanistic basis for As and F^- co-occurrence in Precambrian basement aquifers of Northwest Tanzania and offered insights for groundwater-risk assessment and the design of safe drinking-water supply strategies in mining-affected regions.

1 Introduction

Groundwater is an important freshwater resource and serves as the source of drinking water for about half of the global population (Bhattacharya and Bundschuh, 2015). Reliance on groundwater has increased in recent decades due to pollution and scarcity of surface waters, the impacts of climate variability, and rapid population growth (Ligate et al., 2021; Mosha et al., 2022). Its composition and quality are shaped by the dynamic processes that operate within the Earth's Critical Zone, the near-surface environment where rock, soil, water, air, and living organisms interact over time (Gayathri et al., 2026). Within this zone, lithological structure, weathering intensity, fluid flow, and biogeochemical reactions together control the release, transformation, and transport of dissolved constituents (Chorover et al., 2007). The co-occurrence of arsenic (As) and fluoride (F^-) in groundwater is a direct expression of these coupled processes, and understanding their mobility requires a process-based perspective that links geochemical reactions to weathering environments, hydrogeological settings, and long-term Critical Zone evolution. Persistent challenges to water quality, including geogenic and anthropogenic contaminants and uncontrolled abstraction, have prompted efforts to develop sustainable groundwater exploration and management strategies to ensure drinking water security.

Trace elements in groundwater and surface water can be both beneficial and detrimental to human health and the environment (Bundschuh et al., 2017; Bakyayita et al., 2019). For example, F^- is beneficial at prescribed concentrations (Dissanayake, 1991; Chandrajith et al., 2020). The occurrence of As and F^- in surface and groundwater is a worldwide concern affecting millions of people (Gonzalez-Horta et al., 2015; Podgorski and Berg, 2020; Aullon Alcaine et al., 2020; Irunde et al., 2022). A plethora of As contamination and remediation studies have been reported from Bangladesh, India, Bolivia, Tanzania, and Ghana (Bhattacharya et al., 1997; Ahmed et al., 2024; Maity et al., 2012; Quino-Lima et al., 2020; Bundschuh et al., 2021; Sunkari et al., 2022; Ramos Ramos et al., 2025). On the other hand, the occurrence and remediation of F^- have been reported in India, Ethiopia, Kenya, Tanzania, and Italy (Ijumulana et al., 2020; Ligate et al., 2021; Mridha et al., 2021; Choudhury et al., 2024). The main factors affecting the natural occurrence of As and F^- in groundwater include geology, climate, chemical composition, and residence time (Brunt et al., 2004; Ijumulana et al., 2022). The potential toxicity of As and F^- is dependent on their chemical forms (Reid et al., 2020). The speciation of As and F^- is governed by the environmental geochemical processes within the aquifers, which control their mobility and bioavailability (Alarcón-Herrera et al., 2020). These geochemical processes operate within the broader context of the Critical Zone, the near-surface environment of the Earth where rock, soil, water, air, and biota interact (Chorover et al., 2007; Gayathri et al., 2026). This zone fundamentally regulates the intensity of weathering reactions, the development of reactive mineral surfaces, and the hydrological and geochemical pathways through which trace elements are mobilized or attenuated.

Globally, more than 250 million people are exposed to elevated F^- in drinking water (Patel et al., 2015; Vithanage and Bhattacharya, 2015; Kumar et al., 2016; Kumar et al., 2019; De et al., 2022). In Africa, around fourteen (14) countries, including Tanzania, have drinking water sources with elevated F^- concentrations (Rango et al., 2013; Kimambo et al., 2019; Addison et al., 2020). The elevated concentration of F^- in both groundwater and surface water is dependent on the local geology, mainly governed by the hydrogeochemical processes under favorable conditions such as pH and sufficient concentration of calcium and bicarbonate ions, where F^- leaches into the water through the F^--bearing rocks (Jacks et al., 2005; Vithanage and Bhattacharya, 2015; Kimambo et al., 2019; Addison et al., 2020; Kumar et al., 2024). Furthermore, unmanaged F^--containing materials from anthropogenic sources also contribute to the F^- enrichment in water systems (Rezaei et al., 2017). In the EARV region, about 80 million people are affected by fluorosis, ranging from dental, skeletal, and crippling fluorosis when exposed to F^- concentrations of 1.5–4 mg/L, 4–10 mg/L, and >10 mg/L, respectively, mainly through drinking water (Ghiglieri et al., 2010; Rango et al., 2012; Kaseva et al., 2018; Ijumulana et al., 2022). The presence of As and F^- in groundwater above the Tanzania Bureau of Standard (TBS) and the WHO drinking water guidelines (As >10 µg/L and F^- >1.5 mg/L) in groundwater is a common phenomenon in some regions of Tanzania. This phenomenon poses challenges to the sustainable supply of safe drinking water to the community.

Additionally, the co-occurrence of As and F^- in groundwater represents a major global drinking-water crisis with cascading health and socioeconomic impacts (Centeno et al., 2002; Kapaj et al., 2006; Litter et al., 2019). More than two million people in Tanzania, particularly within the Pangani Drainage Basin (PDV), the Internal Drainage Basin (IDB), and the Lake Victoria Basin (LVB), are at risk of developing all forms of fluorosis because of over-dependence on naturally F^- contaminated drinking water sources (Thole, 2013; Kaseva et al., 2018; Mbabaye et al., 2018; Tomasek et al., 2022; Ijumulana et al., 2022). Therefore, understanding the geochemical processes and spatial variability of the geogenic contaminants (As and F^-) in groundwater resources is essential for resolving the critical challenges of drinking water quality in this region.

The Critical Zone perspective provides a mechanistic framework for linking lithology, climate, and hydrology to groundwater composition and trace element behavior, and it is particularly relevant in tropical and subtropical regions such as the East African Rift Valley (EARV), where intense chemical weathering, complex lithologies, and variable hydrological regimes collectively shape the evolution of groundwater chemistry and the distribution of contaminants (Brantley et al., 2006; Anderson et al., 2007; Maher, 2010; White et al., 2015). Within this framework, variations in mineral composition, water residence time, and redox conditions regulate the release, transformation, and retention of trace elements (Chorover et al., 2007). Applying this approach is particularly useful in the EARV region, where intense weathering, complex geological formations, and highly variable recharge conditions combine to create significant spatial variability in groundwater chemistry. By interpreting As and F^- occurrence within this context, it becomes possible to better explain their co-mobilization and to identify the key controls on their distribution (Brantley et al., 2006; Maher, 2010; White et al., 2015). Building on the Critical Zone framework, this study investigated how geological settings, weathering processes, and hydrological pathways collectively influence the spatial variability, mobilization, and co-occurrence of As and F^- in groundwater systems of the Geita district in Northwestern Tanzania.

This study aims to delineate the hydrogeochemical characteristics of groundwater used for community drinking water supply in the Geita district of Northwestern Tanzania and to identify the geochemical controls on the spatial distribution and co-occurrence of As and F^-. The study adopted a Critical Zone perspective, in which interacting geological, weathering, and hydrological processes regulate porosity and permeability, create reactive mineral surfaces, and establish pH and redox conditions that influence the mobility of trace elements. Within this framework, variations in mineral composition, water residence time, and flow paths are expected to modulate reaction progress and solute release, shaping groundwater chemistry across the landscape. Specifically, the study seeks to characterize the physicochemical properties and major ion composition of groundwater from shallow wells and boreholes, determine hydrogeochemical facies and dominant water types, quantify spatial autocorrelation and clustering of key parameters, evaluate the saturation states of minerals relevant to As and F^- mobility, and assess the co-occurrence and spatial variability of these contaminants in order to support risk assessment and the design of safe water supply strategies.

2 Study area

2.1 General description

This study involved sixteen (16) administrative wards (Buhalahala, Bukoli, Bulela, Bung'wangoko, Busanda, Kamena, Kalangalala, Kanyara, Kasamwa, Lwamgasa, Mtakuja,

Nyakamwaga, Nyanguku, Nyankumbu, Nyarugusu and Shiloleli) in Geita district within the Geita region of the Lake Victoria Basin, Northwestern Tanzania (**Fig. 1**). Geita district is characterized by an equatorial hot and humid climate with a bi-modal rainfall pattern experiencing precipitation during the months of March to May and October to December (FDMT, 2016). The mean annual rainfall in the lowlands of Geita region ranges between 900 and 1,100 mm and temperature ranges between 14 and 28°C. The mean annual evaporation is 2,100 mm. The region is characterized by a flat topography dominated by open grassland and wetland. The topography of the study area ranges between 1,148 and 1,588 m above mean sea level (**Fig. 1**). The favorable climatic conditions for agriculture and livestock keeping and the abundance of natural resources have supported the rapid population growth in the LVB, accounting for over 26% of the national population (UNEP, 2006; URT, 2013). Earlier studies by Kassenga and Mato (2008) and Almås and Manok (2012) reported an elevated concentrations of As and mercury (Hg) in groundwater sources, indicating potential health risks to the surrounding communities. Nyanza et al. (2019) highlighted severe public health concerns, particularly among pregnant women exposed to elevated levels of As and Hg through drinking water, especially in populations residing near the artisanal and small-scale gold mining areas.

2.2 Geology and hydrogeology

The geological environment of the study area is heterogenous, consisting mainly of volcanic-sedimentary and migmatite-granitoid metasedimentary complexes (Ikinguraa et al., 2006; Henckel et al., 2016; Lucca, 2017; Ligate et al., 2022). Young alluvial and eluvial sediments are the characteristic of low-lying terrains (**Fig. 2**). The lithology and degree of weathering of the parent rocks exert a fundamental control on aquifer porosity, permeability and the mineralogical composition of the weathering profile, which together influence the groundwater flow dynamics and geochemical evolution. These weathering profiles develop within the Critical Zone, the near-surface environment where rock, soil, water, air, and biota interact and ultimately shaping the hydrogeochemical characteristics of the groundwater systems.

The dominant water-bearing units include fractured and weathered basement rocks of the Precambrian Craton and Tertiary-Quaternary unconsolidated sediments, underlain by the heterogeneous bedrock formations (Fernandes et al., 2013). Macdonald et al. (2012) reported that shallow aquifers in many sub-Saharan African rural settings are typically discontinuous, with yields ranging from 0.5 to 2 L/s. In contrast, high-yielding aquifers are associated with thick alluvial deposits and Quaternary sediment composed of sand

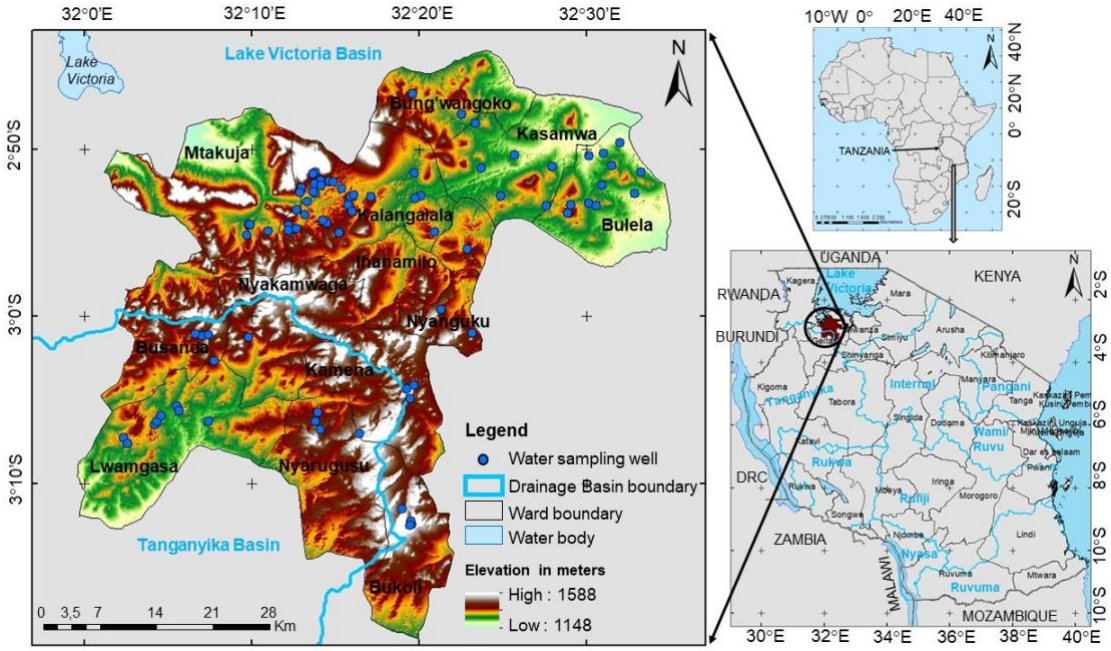

Figure 1. *Map of the study area in Geita district, located at the boundary between the Tanganyika and Lake Victoria Basins in Northwest Tanzania, showing groundwater sampling locations, ward boundaries, drainage basin limits, surface water bodies, and elevation range of the study site. Blue circles indicate sampled wells. The digital elevation model highlights topographic variability across the area, and inset maps illustrate the regional setting within Tanzania and East Africa.*

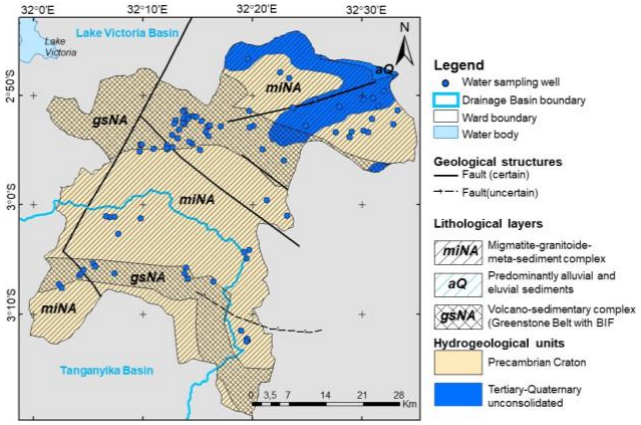

Figure 2. *Geological and hydrogeological map of Geita district showing lithological units, hydrogeological formations, structural features, and groundwater sampling locations within the Lake Victoria goldfields. The map highlights migmatite granitoid meta sediment complexes, volcano sedimentary Greenstone Belt units, alluvial and eluvial sediments, Precambrian Craton formations, and Tertiary Quaternary unconsolidated deposits. Fault traces and drainage basin boundaries are also indicated. Data sources include hydrogeological data (BGS, 2019) and geological data (TGS, 2018).*

and gravel, particularly near the shores of Lake Victoria (Cook et al., 2016). Groundwater recharge in both shallow and deep aquifers occurs through the fractured zones of the Precambrian Craton. The unconsolidated sediments commonly form the perched shallow aquifers overlying the weathered bedrock.

Most of the communities in the study area get access to groundwater from the hand dug shallow wells (SW, <25 m) and machine drilled boreholes (BH, >25 m). However, the seasonal variability strongly affects the yield of most shallow aquifers, leading to water scarcity is some communities during the dry season (Henckel et al., 2016).

3 Materials and methods

3.1 Water sampling and measurement of in-situ parameters

Water sampling was carried out during the dry season in August 2018 (**Figs. 1 and 2**). A total of 88 groundwater samples were randomly collected from SW (n = 42) and BH (n = 46) used as a source for drinking water and other domestic purposes mainly in the rural settings. Before sampling, the wells were purged adequately, at least three minutes to ensure that the sampled water is a true representative of the groundwater in the wells. All samples were collected directly from the source by using 1L iodine-free polyethylene bottles. In-situ field parameters including water temperature (T), pH, redox potential (Eh) electrical conductivity (EC), and total dissolved solids (TDS) were measured by using HQ40D Hach® potable water quality multimeter calibrated each day before the field measurement. F^- was measured by the fluoride selective electrode at Ngurdoto Defluoridation Research Centre (NDRC). The location of the sampling sites was recorded using a hand-held global positioning (GPS) receiver Global Mapper 20. The Hach As low-range test kit (0–500 µg/L) was used at each water source for the in-situ estimation of total As concentrations (Rahman et al., 2002; Stolze et al., 2022), the typical procedures involved the reduction in inorganic As to arsine gas that react with mercury bromide impregnated onto the test strip to form a mixture of arsenic and halogen. The halogen subsequently discolors the test strip the degree that is proportional to the total As concentration in the sample. Furthermore, As speciation was carried out in the field by using disposable cartridges (Disposable Cartridges®, Metal Soft Centre, USA). For As speciation, 50 mL of groundwater was passed through a cartridge packed with 2.5 g of selective adsorbent called aluminosilicate at the flow rate of about 50 mL per minute using a 50 mL syringe. As(V) in water samples was adsorbed by the aluminosilicate and As(III) was retained in the filtrate. The average recovery of As(III) in the filtrate was 95% (recovery range is 93–104%) (EPA, 2017; Lucca, 2017). The pH of water samples was within the range of 4 to 9, that range was ideal for the effectiveness of the method. The collected filtrate was then transported to the laboratory for analysis using Inductively Coupled Plasma-Optical Emission Spectrometry (ICP-OES). Groundwater samples collected for laboratory analysis included: (a) 500 mL filtered (using Sartorius 0.45 µm filters) for major anions; and (b) 500 mL filtered and acidified using a few drops of 70% nitric acid (HNO_3) to pH less than 4 for major cations and trace elements including As. All field instruments were calibrated as per the manufacturer's guidelines (EPA, 2017).

3.2 Chemical analysis

The concentration of major anions; Cl^-, SO_4^{2-}, HCO_3^-, and NO_3^- were measured at the Environmental Laboratory of the Government Chemist's Laboratory Authority (GCLA) using Dionex DX-120 Ion Chromatography (IC). Major cations (Ca^{2+}, Na^+, K^+, and Mg^{2+}), and TEs, viz. aluminum (Al), boron (B), barium (Ba), copper (Cu), iron (Fe), lithium (Li), manganese (Mn), nickel (Ni), zinc (Zn) and As were analyzed by ICP-OES (Thermo Scientific iCAP 6000 Series) at the GCLA in Tanzania.

3.3 Precision, quality control, and quality assurance

Containers and bottles used during sampling, storage, transportation, and measurements of water samples were washed with dilute nitric acid (HNO_3) and rinsed with deionized water. The accuracy and precision were regularly checked by the laboratory's internal quality control. The quality assurance of results of major ions analysis was checked through the calculation of the charge balance error. The blank samples for both field and laboratory analyses were prepared and analyzed according to the standard procedures. The analytical accuracy of the measurement from ICP-OES was checked by using certified reference material (NIST SRM 1640a-the trace elements in natural waters), and the recovery for the analyzed TEs was within the acceptable range of 95–105% following the US EPA standard guidelines (EPA, 2007). In all cases, replicate analysis was performed to check the reproducibility of the analysis and the precision and accuracy of the results.

3.4 Statistical analysis

The statistical analysis was carried out using the IBM SPSS Statistics (version 28) to understand the occurrence and distribution of major ions, As, F^-, and other TEs in the groundwater samples. The statistical tests considered in this study include the normality test, descriptive statistics (minimum, maximum, mean, and standard deviation), and multivariate statistical analysis. All parameters in water samples were subjected to normality tests and correlation analysis to understand the degree of dependence among them at a 0.05 significance level. Cluster analysis (CA) was performed to classify parameters by using a hierarchical agglomeration on the normalized data by Ward's method using squared Euclidean distances as a similarity measure (Marinovic Ruzdjak and Ruzdjak, 2015).

3.5 Spatial analysis

The geostatistical techniques were used to ascertain the statistical distribution and spatial variability of major ions, As, F^- and other TEs in the study area. Exploratory spatial data analysis was performed on the physicochemical and geochemical data of water samples collected from the study area. The Sharpiro-Wilk statistical test was used to ascertain the normality in the observed values at a 0.05 significance level. On the other hand, Levene's test was used to understand the homogeneity of variance. The univariate global Moran's I statistical method used for spatial autocorrelation analysis in water quality parameters.

3.6 Geochemical modeling

The geochemical modeling involved the determination of the distribution of chemical species in water samples at thermodynamic equilibrium. Analytical data of groundwater samples were subjected to Visual MINTEQ geochemical code. More than 20 thermodynamic codes are available including Geochemist's Workbench (GWB) and PHREEQC/PHREEPLOT, and Visual MINTEQ (Jacks and Nystrand, 2019; Gustafsson, 2022). In this study, the geochemical equilibrium model Visual MINTEQ, version 3.1 (Gustafsson, 2022) was used to model the saturation index to determine the possible mineral equilibria with regard to As and F^- in groundwater samples.

4 Results and discussion

4.1 Physicochemical characteristics

The physicochemical parameters of the water samples from SW and BH are presented in **Table 1**. Groundwater temperature ranged between 23.1 and 29.6°C (mean: 26.3°C) and between 23.9 and 28.7°C (mean: 26.4°C) in SW and BH samples, respectively. The temperature variation was not significant ($p > 0.05$) between SW and BH samples during the dry season compared to the wet season, which is typical for regions with tropical climate conditions.

The groundwater pH in SW showed wide variability between 5.7 and 7.4 (mean: 6.7), similarly the BH groundwater exhibited a relatively wide range of variation between 5.9 and 7.5 (mean: 6.8). On the other hand, the Eh ranged between 213 and 501 mV (mean: 415.9) and between 100 and 535 mV (mean: 404.2) for SW and BH, respectively. The EC in the SWs also indicated a wide range of variability between 60 and 1,364 µS/cm (mean: 270 µS/cm) which is comparable to other literature within the study area (Almås and Manoko, 2012; Ijumulana et al., 2017). In the BH samples, the EC values ranged between 71.4 and 1,971 (mean: 466 µS/cm). The TDS values ranged between 31.8 and 722.9 mg/L (mean: 149.4 mg/L) and between 50 and 1,084.1 mg/L (mean: 272.9 mg/L) in SW and BH, respectively. Compared to the WHO and TBS recommend provisional guideline values of 400 µS/cm and 300 mg/L for EC and TDS, respectively the two groundwater sources indicated the good water quality for drinking purposes.

4.2 Major ion concentrations

The major ion concentration of the groundwater is summarized in **Table 2**. Considerable variation was observed in the concentration of major cations in the SW and the BH water sources. In SW, Ca^{2+} and Na^+ were

Table 1. *Physicochemical characteristics in shallow wells (SW, n = 42) and boreholes (BH, n = 46) samples from Geita district, Northwestern Tanzania. Classification of SW and BH was based on depth to groundwater whereby all SW had a depth <25 m and BH had a depth <25 m and BH had a depth of >25 m (MacDonald et al., 2012).*

Parameter	Minimum	Maximum	Q1	Median	Q3	IQR	Mean	s.d.
Shallow wells								
Altitude (m)	1,192	1,316					1,256	
T (°C)	23.1	29.6	25.5	26.5	27.2	1.7	26.3	1.4
pH	5.7	7.4	6.4	6.7	7.0	0.6	6.7	0.5
EC (µS/cm)	60	1,364	119.4	187.9	341	221.6	270.3	243.1
Eh (mV)	213	501	391	433	461	70.0	415.9	64
TDS (mg/L)	31.8	722.9	65.7	104.2	180.7	115.1	149.4	132.6
Boreholes								
Altitude (m)	1,181	1,390					1,263	
T (°C)	23.9	28.7	25.5	26.2	27.2	1.7	26.4	1.2
pH	5.9	7.5	6.6	6.9	7.2	0.7	6.8	0.4
EC (µS/cm)	71.4	1,971	174	286.5	739	565	466.2	466.2
Eh (mV)	100	535	397	427.5	460	63	404.2	85.4
TDS (mg/L)	50	1,084.1	92.6	162.5	391.7	299.1	272.9	248.1

predominant with concentrations ranging between 4 and 74.6 mg/L and 2.1 and 62.3 mg/L, respectively. The Mg^{2+} was the third predominant cation, with concentrations ranging between 0.1 and 38 mg/L, while K^{+} was the least prevalent major cation in water, ranging between 0.1 and 35.6 mg/L. The variation of major cations in BH followed a similar trend with Ca^{2+} and Na^{+} as abundant cations, ranging between 1.1 and 72.8 mg/L and 2.2 and 102 mg/L, respectively, followed by Mg^{2+} with concentrations between 0.1 and 15.8 mg/L. Likewise, the K^{+} was the least prevalent major cation in water, ranging between 0.03 and 6 mg/L (**Table 2**). The variability of Ca^{2+} and Mg^{2+} was similar with samples from Geita town having relatively lower concentrations as compared to those from Geita rural. The differences in the concentration of major cations can be explained by the difference in source rocks and conditions for weathering as well as the subsequent dissolution process.

The most abundant anion in SW was HCO_3^{-} with concentrations ranging between 13.2 and 322.4 mg/L followed by SO_4^{2-} and Cl^{-} with concentrations between 0.1 and 131.4 mg/L and between 3 and 55.5 mg/L, respectively. The abundance of major anions in BH was also dominated by HCO_3^{-}, SO_4^{2-}, and Cl^{-} in that order with concentration between 15.2 and 257.8, 0.4 and 128.3, and 0.4 and 104.9 mg/L, respectively. The enrichment of major anions in groundwater is mainly geogenic. However, the Cl^{-} enrichment in groundwater can be originating from both geogenic and anthropogenic sources, especially for the wells that were not properly protected by encasing with concrete (or other protective materials) to prevent seepage of contaminants such as sewage and other domestic wastes. The concentration of NO_3^{-} in SW and BH ranged between 0.10 and 19.81 mg/L and 0.04 and 16 mg/L, respectively. The mean concentration in the two drinking water sources was below the maximum allowable concentration of 50 mg/L recommended by the WHO (WHO, 2017). In groundwater, NO_3^{-} is usually associated with anthropogenic sources. The concentration between 3.1 and 10 mg/L provides an indication of pollution emanating from anthropogenic activities (Patel et al., 2015). The detailed hydrogeochemical facies, processes, and water type, are summarized in the Durov plots (**Fig. 3**).

The hierarchical cluster dendrogram reveals two groups of water quality parameters for both SW and BH samples in the Geita region (**Fig. 4**). Group I represent the correlations among different parameters, namely pH and T, major ions (Na^{+}, K^{+}, Ca^{2+}, Mg^{2+}, SO_4^{2-}, NO_3^{-}, and Cl^{-}), and trace elements (As and F^{-}), while Group II is represented by EC

Table 2. *Summary statistics of major ions concentrations (mg/L) in SW (n = 42) and BH (n = 46) samples from Geita district, Northwestern Tanzania.*

Parameter	Minimum	Maximum	Q1	Median	Q3	IQR	Mean	s.d.
Shallow wells								
HCO_3^-	13.2	322.4	37.1	48.4	88.2	51.1	80.4	74
Cl^-	3.0	55.5	10.4	18.6	32.8	22.4	22.3	14.1
SO_4^{2-}	0.1	131.4	2.6	5.2	11.5	9.0	15.7	29.9
NO_3^-	0.1	19.81	0.58	1.1	5.05	4.47	3.1	4.4
Na^+	2.1	62.3	8.9	18.8	32.3	23.4	43.2	16.0
Mg^{2+}	0.1	38	0.5	1.0	2.7	2.2	3.7	7.1
K^+	0.1	35.6	0.6	1.8	4.0	3.3	3.6	5.9
Ca^{2+}	4.0	74.6	9.2	17.2	24.8	15.6	18.9	13.7
Boreholes								
HCO_3^-	15.2	257.8	49.1	64.2	116.1	66.9	86.2	55.6
Cl^-	0.4	104.9	8.5	13.6	25.0	16.5	21.5	22.8
SO_4^{2-}	0.4	128.3	2.7	9.2	15.6	13	12.7	19.6
NO_3^-	0.04	16	0.7	1.25	2.1	1.4	2.7	3.8
Na^+	2.2	102.1	12.2	20.7	30.2	17.9	25	18.2
Mg^{2+}	0.1	15.8	1.7	4.0	6.6	4.9	4.8	3.9
K^+	0.03	6.0	0.3	1.0	1.9	1.6	1.4	1.3
Ca^{2+}	1.1	72.8	8.3	13.1	22.1	13.9	18.7	16.5

and TDS. This indicates that As and F^- enrichment is associated with coupled physicochemical processes in the aquifer system rather than simple salinity effects. This grouping reflects interactions among mineral weathering, ion exchange, and redox conditions within the near-surface weathering profile, which together regulate the mobility of As and F^- in groundwater.

4.3 Trace element concentrations

The concentrations (in µg/L) of TEs that are essential for human health including Al, B, Ba, Cu, Fe, Li, Mn, Ni, and Zn in water samples were below the drinking water quality guidelines based on WHO and TBS in both SW (*n* = 10) and BH (*n* = 7) (**Tables S1 and S2**). Al concentration ranged between 11.57 and 1,252.54 (mean: 161.12) and between 13.35 and 2,047.63 (mean: 315.56) in SW and BH, respectively. The B concentrations were ranged between 4.17 and 138.32 (mean: 20.32) in SW while it varied between 1.94 and 17.22 (mean: 8.45) in BH. On the other hand, Ba ranged between 26.14 and 478.11 (mean: 150.01) in SW while it ranged between 18.12 and 164.28 (mean: 71.59) in BH. Cu values ranged between 0.89 and 268.17 with a mean of 29.96 and between 0.75 and 13.02 with a mean of 4.56 in SW and BH, respectively. Iron (Fe) concentration varied from 2.56 to 1,992.53 and 9.88 to 6,312.78 in SW and BH, respectively. Fe is the most important cation associated with the As in the aquifers because under favorable redox conditions As may precipitate or dissolve hence controlling its availability in drinking water samples. Li concentration was in the range from 0.42 to 21.38 (mean: 7.31) and 0.97 to 15.35 (mean: 5.27) in SW and BH, respectively. The values for Mn, Ni and Zn were in the range from 1.06 to 1,303.16 (mean: 190.10), 0.29 to 525.86 (mean: 53.86) and 5.61 to 3,742.09 (mean: 391.89) respectively in SW and 2.01 to 761.46 (mean 170.82), 0.28 to 6.86 (mean: 1.95) and 5.77 to 90.09 (mean: 21.77) respectively in BH. The correlation matrix revealed statistically significant relationships among several trace elements ($p < 0.05$; **Tables S3 and S4**), indicating shared sources and coupled geochemical behavior.

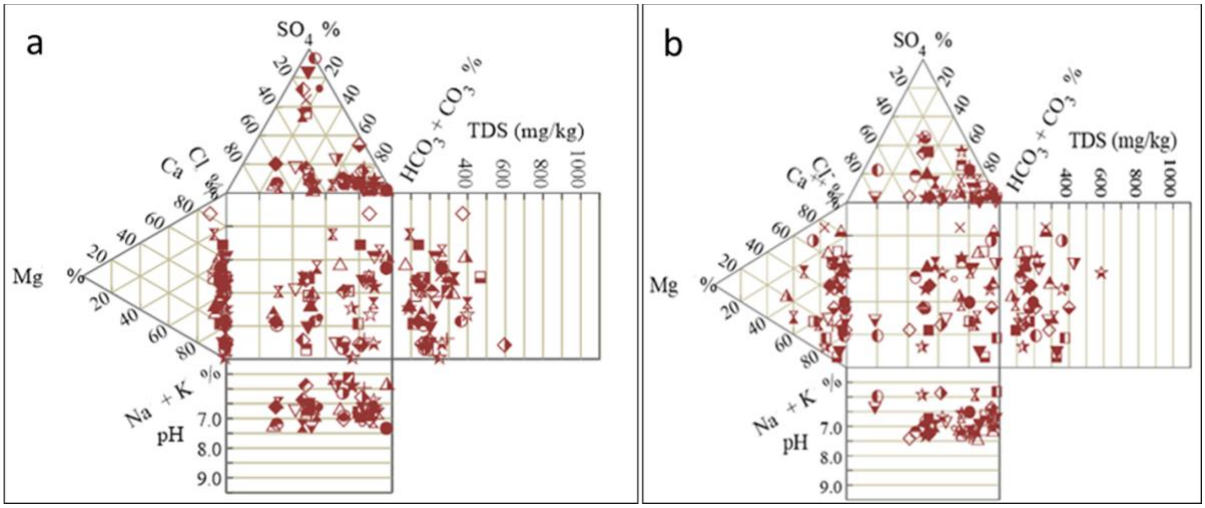

Figure 3. *Durov diagrams illustrating hydrochemical facies and the distribution of major ions, pH, and total dissolved solids in groundwater samples from (a) shallow wells (SW) and (b) boreholes (BH) in the Geita district. The plots indicate dominant Ca-HCO_3 and Na-HCO_3 water types, reflecting varying degrees of water rock interaction, ion exchange, and residence time within the aquifer system, with Na-HCO_3 facies associated with elevated fluoride concentrations.*

The observed variability in concentrations and inter-element correlations reflects differences in lithology, weathering intensity, and redox conditions, together with ion exchange and mineral transformation processes operating within the aquifer system.

F^- concentration ranged between 0.13 and 1.34 (mean: 0.34 mg/L) and between 0.20 and 2.17 (mean: 0.75 mg/L) in SW and BH, respectively (**Table 3**). Total As concentration ranged between 10 and 280 (mean: 95 µg/L) and between 2.5 and 250 (mean: 85 µg/L) in SW and BH, respectively. Most of the total As concentrations were found to be As(V) and only showed minor fractions of As(III) concentration which ranged between 2.3 and 5.63 (mean: 4.25 µg/L) and between 0.92 and 5.52 (mean: 4.05 µg/L) in SW and BH, respectively.

4.4 Statistical distribution of physicochemical parameters

The cumulative statistical distribution functions indicated non-normal distribution in most physiochemical parameters in both SW and BH (**Figs. 5 & 6**). The Sharpiro-Wilk test statistics (W) were statistically significant (at a 0.05 significance level), indicated by * in the figures, for all parameters except for temperature in SW. Furthermore, the Levene's test for homogeneity of variance indicated instability in concentrations for some parameters (**Tables**

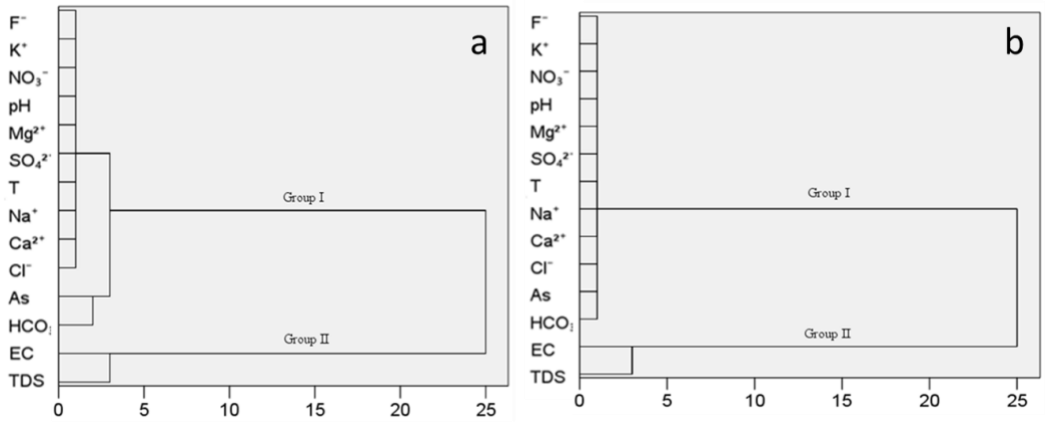

Figure 4. *Hierarchical cluster dendrogram showing relationships among physicochemical parameters, major ions, arsenic, and fluoride in groundwater samples from (a) shallow wells (SW) and (b) boreholes (BH) in the Geita district. Two main groups are identified, reflecting associations between trace elements and major ions, and the influence of dissolved solids on overall water chemistry.*

Table 3. *Summary statistics of F^-, As(T), and As(III) in SW (n = 42) and BH (n = 46) samples from Geita district, Northwestern Tanzania.*

Parameter	Min	Max	Q1	Median	Q3	IQR	Mean	s.d.
Shallow wells								
F^- (mg/L)	0.13	1.34	0.23	0.32	0.45	0.22	0.38	0.24
As(T) (µg/L)	10	280	50	70	150	100	95	70
As(III) (µg/L)	2.3	5.63	3.91	4.25	5.01	1.1	4.25	0.85
Boreholes								
F^- (mg/L)	0.2	2.17	0.28	0.45	1.09	0.81	0.75	0.6
As(T) (µg/L)	2.5	250	30	70	100	70	85	69
As(III) (µg/L)	0.92	5.52	3.40	4.25	4.61	1.2	4.05	1.02

S5–S7). Apart from the EC, which demonstrated a statistically significant variance, the rest of the parameters indicated constant variance in their concentrations across the study area. All the major ions indicated constant variance in their concentrations across the study area. However, F^- showed statistically significant variance in their concentrations across the study area.

The mean pH values are within the recommended standard values for drinking water purposes according to WHO and TBS guidelines. The pH has a significant influence on water quality. The variability of pH significantly affects the geochemistry of groundwater where the low pH (<5) is favorable for the dissolution of As(III) from parent materials and the reduction of As(V) to As(III), at high pH (~8 to 9) there is competitive adsorption between As(V) and OH^- ions rendering As availability in groundwater. At relatively higher pH (>8), F^- enrichment in groundwater is favored through ion exchange reactions with OH^-, and the presence of sufficiently high concentrations of HCO_3^- and Na^+ has also been shown to favor the release of F^- from parent minerals into groundwater in the aquifers (Singh et al., 2011). In groundwater, the pH is mainly controlled by the chemical species in both the water and solid matrix. In surface water the composition of water is determined by many factors both from natural (e.g., decomposition of organic matter) and anthropogenic sources, these, in turn, can affect the pH of water (Tibebe et al., 2022).

High TDS and EC levels affect the taste (salty) and color (brownish/brackish) of the water. On the other hand, extremely low TDS and EC values are indicators of a shortage of essential minerals such as Ca^{2+}, Na^+, Mn, and Se. Overall, the mean EC and TDS values were below the guideline values suggested by the WHO and TBS for drinking water purposes. In comparison with the water salinity classification system based on the TDS levels, established by Kumar et al. (2024), all water samples were non-saline. Both TDS and EC are dependent on the dissolved salts/minerals in the water. Although there is no direct human health effect associated with EC and TDS in drinking water, high and extremely low levels may be objectionable to consumers owing to aesthetic values such as color and taste.

One-way Kruskal-Wallis test indicated significant variance for some water quality parameters in SW and BH (**Table S8**). Mean concentrations differed significantly only for the EC and TDS in the physicochemical parameters category whereas none of the mean concentrations in the major anions differed significantly in the two drinking water sources. For the major cations, the mean concentrations differed significantly for the Mg^{2+} and K^+ concentrations. While for the trace elements, only the mean concentrations in F^- differed significantly. The mean concentrations of As did not differ significantly among the two drinking water sources. The test statistics for the field and laboratory-measured concentrations were the same (**Fig. 7**). Since the water samples analyzed in the laboratory were obtained from the speciated samples using As speciation cartridges, the observed low concentration As(III) in the laboratory-analyzed samples could be due to oxidation and precipitation on the Fe oxyhydroxide surfaces. In addition, As concentrations measured in the field correlated exponentially with those measured in the laboratory. This correlation persisted for all samples when combined and in SW and BH (**Fig. 7**).

4.5 Geochemical characteristics of arsenic and fluoride in groundwater

Geochemical modeling of As and F^- was performed by calculating the saturation index of different As and F^-

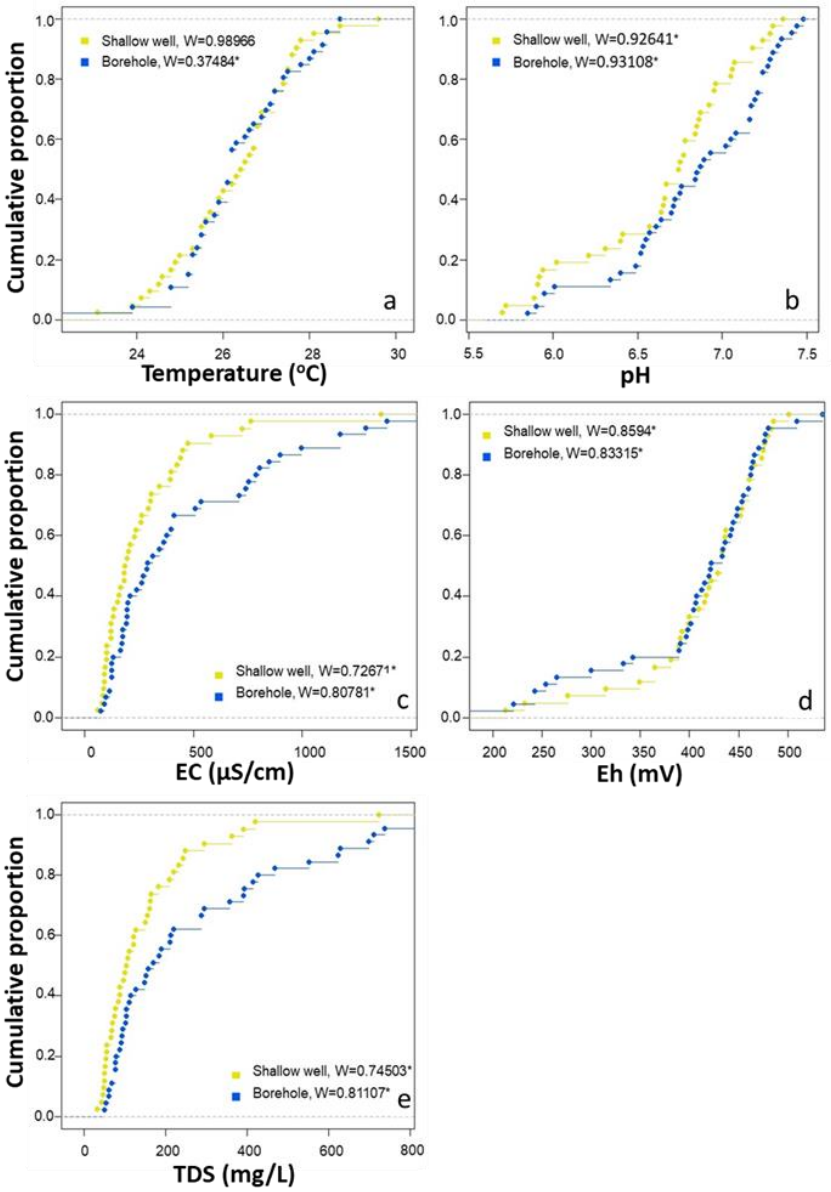

Figure 5. *Statistical distribution of the physiochemical parameters (a–e) in drinking water sources of Geita district within the major Gold Fields in Northwestern Tanzania. The inferential statistical test was based on the Shapiro-Wilk test for normality in the concentrations of each parameter in shallow wells (SW) and boreholes (BH). The significance level was 0.05. W stands for the test statistic used while * signifies the non-normality in the parameter concentration.*

containing minerals such as ferrihydrite, arsenopyrite, calcite, and fluorites by using Visual MINTEQ and geochemical codes. Field-measured values for pH, HCO_3^- alkalinity, and temperature were used. The results showed that important minerals such as goethite, ferrihydrite, and montmorillonite are oversaturated and hence they can co-precipitate with As, and dissolution of the same may occur under favorable pH and redox conditions (**Fig. S1**). Both fluorite and calcite were undersaturated in all water samples (**Fig. S2**). In the context of the Critical Zone, these saturation conditions indicate evolving reactive surfaces (Fe oxyhydroxides, clays, and carbonates) that regulate adsorption–desorption and buffering, while Ca availability and ion exchange shift equilibria toward F^- release in alkaline Na–HCO_3 waters. The Ca-HCO_3 water type shows very low concentrations of F^- as compared to the Na-HCO_3 water type because soluble F^- in groundwater of the former type is independent of the dissolution of fluorite minerals. It can therefore be deduced that the extent of the solubility of fluorite and calcite minerals is responsible for the control of water composition in the aquifers (Rafique et al., 2009). The previous literature has shown that F^- enrichment in groundwater is associated with Na-rich and Ca-poor alkaline water whereby dissolution of fluorite and other F^- containing

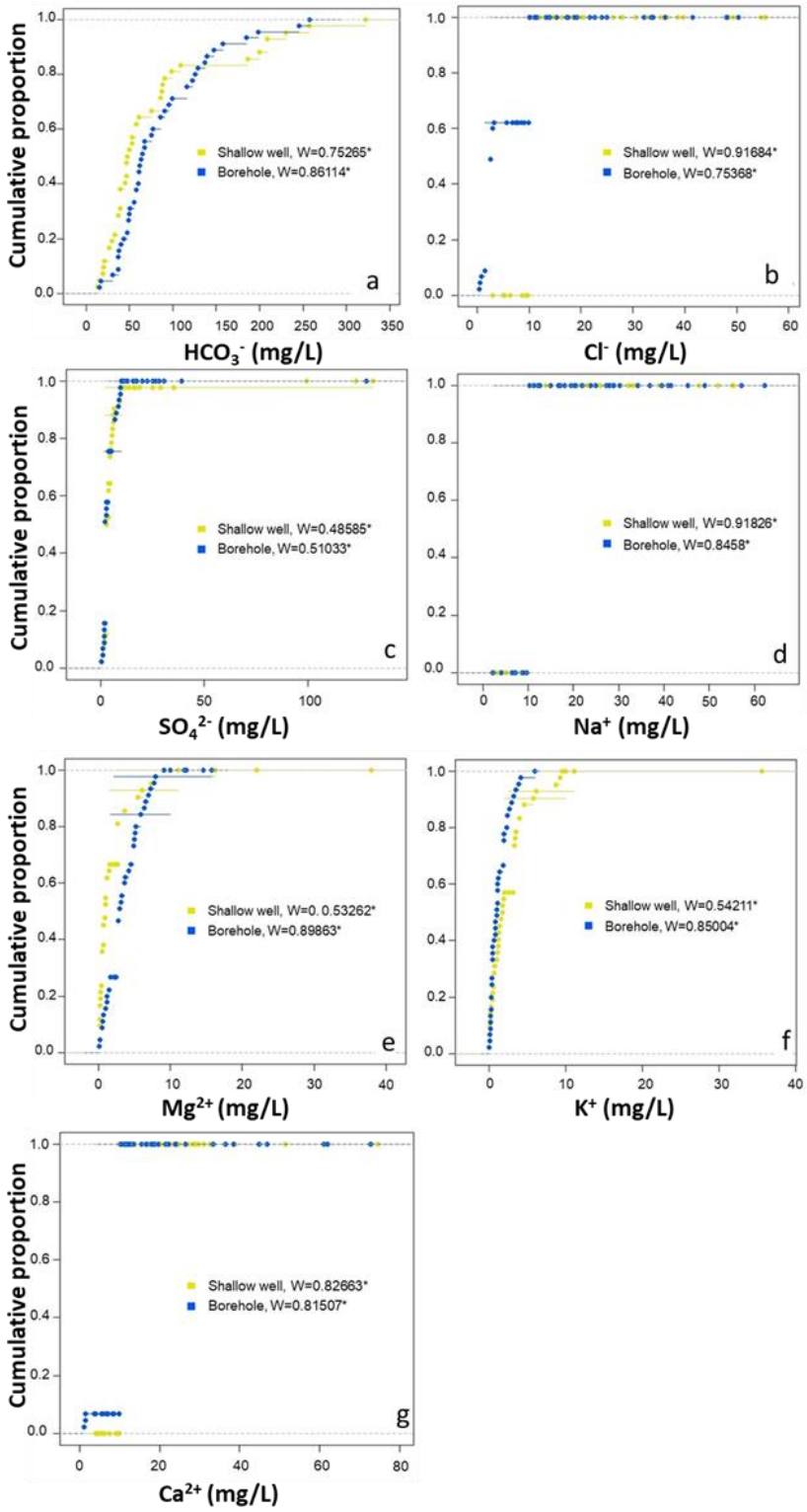

Figure 6. *Statistical distribution of the anions (a–c) and cations (d–g) concentrations in drinking water sources of Geita district within the major Gold Fields in Northwestern Tanzania. The inferential statistical test was based on the Shapiro-Wilk test for normality in the concentrations of each parameter in shallow wells and boreholes. The significance level was 0.05. W stands for the test statistic used while * signifies the non-normality in the parameter concentration.*

minerals, competitive adsorption of co-occurring anions and cation exchange in the aquifers (Brunt et al., 2004; Kimambo et al., 2019; Xing et al., 2022). The mobilization of As can also be explained by the oxidizing conditions that favor the

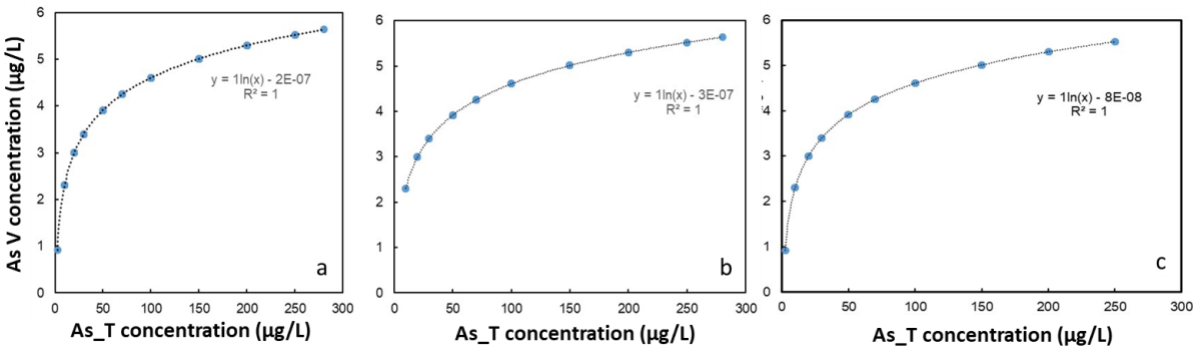

Figure 7. *Correlation between field measured and laboratory analyzed As(T) (total As) concentrations in (a) all water samples, (b) shallow wells (SW), and (c) boreholes (BH) used as water sources for drinking water and other domestic activities in Geita district.*

desorption of As from Fe-oxyhydroxides (hematite and goethite). The characteristic alkaline (pH above 7) conditions result in negatively charged minerals surfaces, which subsequently limits the adsorption of As species and makes them available in solution. However, other factors such as the contact time flow dynamics, and microbial activities also affect the As and F^- dissolution. Overall, the elevated concentrations of As and F^- as reported in the groundwater samples are mainly from geogenic sources.

4.6 Spatial autocorrelation in drinking water quality parameters

Geospatial analysis indicated that among the physicochemical parameters, only temperature showed spatial randomness having z-value of 1.1697 (*p*-value = 0.129). Although significant, the strength of the significance varied between other physicochemical parameters (**Table 4**). The strength was the highest for pH (z-value = 7.6272; *p*-value = 0.001) followed by TDS, EC, and Eh. This spatial signal is consistent with Critical Zone frameworks, where contrasts in permeability, fracture density, and flow pathways modulate fluid residence time and the extent of weathering reactions that set pH, EC, TDS, and redox conditions. On the other hand, only K^+ demonstrated a significant spatial clustering pattern as verified by the large z-value (4.2742) and the small *p*-value (0.001) in the major ions category. Except for NO_3^-, all parameters in the category of health concerns (As and F^-) also demonstrated spatial clustering. However, the strength of the spatial dependence varied among the parameters. The global Moran's I indicated the clustering pattern in some of the drinking water quality parameters. The univariate local Moran's I further identified and mapped specific locations where similar values grouped together, revealing areas where drinking water sources had consistently high and low concentrations.

The drinking water sources with high pH dominated the northern part of the study area (**Fig. 8a**). The lithological units in this part included the volcano-sedimentary complex (Greenstone Belt with BIF) and migmatite-granitoid-meta-sediment complex in the south and north sections, respectively. The slope in the two sections was relatively flat with the lowest slopes dominating the north section. On the other hand, the drinking water sources with low pH dominated the southern part of the study area. The majority of drinking water sources in this part were in the volcano-sedimentary complex (Greenstone Belt with BIF) at relatively steep slopes where the small-scale and artisanal gold mining activities are in full swing. High values of EC (**Fig. 8b**) and TDS (**Fig. 8d**) in the drinking water sources dominated the northern part of the study area within the migmatite-granitoid-meta-sediment complex. On the other hand, the majority of the drinking water sources with low values are concentrated in the volcano-sedimentary complex (Greenstone Belt with BIF) mainly in the relatively elevated slopes characterized by the high population density and small-scale mining activities. The Eh did not demonstrate clear distinct spatial patterns (**Fig. 8c**) except for the high spatial pattern that dominated the southern part of the study area. The northern part demonstrated heterogeneity as envisaged by many high values together with low values. The drinking water sources with high concentrations of K^+ were scattered in the study area where most of the sources (7 out of 10) observed in the volcano-sedimentary complex (Greenstone Belt with BIF) (**Fig. 8e**). The drinking water sources with relatively low concentrations dominated the north and south of the study area. The low concentration in the northern part was mainly in the lowlands whose lithology

Table 4. *Summary of spatial autocorrelation analysis in drinking water quality parameters considered in this study.*

Parameter	Moran's I	E[I]	Mean	s.d.	z-value	*p*-value
Temperature	0.0306	-0.0115	-0.0121	0.0365	1.1697	0.129
pH	0.5098	-0.0115	-0.0124	0.0685	7.6272	**0.001**
EC (µS/cm)	0.1880	-0.0115	-0.0117	0.0653	3.0581	**0.007**
Eh (mV)	0.1191	-0.0115	-0.0114	0.0641	2.0343	**0.029**
TDS (mg/L)	0.2251	-0.0115	-0.0113	0.0658	3.5945	**0.001**
HCO_3^- (mg/L)	0.0150	-0.0115	-0.0096	0.0686	0.3587	0.341
Cl^- (mg/L)	-0.0595	-0.0115	-0.0093	0.0658	-0.7623	0.221
SO_4^{2-} (mg/L)	0.0383	-0.0115	-0.0130	0.0628	0.8164	0.174
Na^+ (mg/L)	0.0416	-0.0115	-0.0100	0.0658	0.7828	0.214
Mg^{2+} (mg/L)	-0.0032	-0.0115	-0.0081	0.0655	0.0746	0.421
K^+ (mg/L)	0.1971	-0.0115	-0.0128	0.0491	4.2742	**0.001**
Ca^{2+} (mg/L)	-0.0227	-0.0115	-0.0134	0.0658	-0.1424	0.465
F^- (mg/L)	0.4257	-0.0115	-0.0150	0.0655	6.7261	**0.001**
As(T) (µg/L)	0.2979	-0.0115	-0.0140	0.0667	4.6772	**0.001**
As(III) (µg/L)	0.4542	-0.0115	-0.0146	0.0653	7.1817	**0.001**
NO_3^- (mg/L)	0.0916	-0.0115	-0.0122	0.0705	1.4743	0.077

is dominated by the migmatite-granitoid-meta-sediment complex together with alluvial and eluvial sediments.

These lithology-slope-recharge patterns indicate that Critical Zone processes, such as profile thickness, fracture-focused recharge, and variable residence time, govern the evolution of alkalinity and redox state, thereby controlling trace-element behavior (Brantley et al., 2006; Chorover et al., 2007; Brooks et al., 2015).

4.7 Critical Zone controls on As and F^- mobility

Both F^- (**Fig. 8f**), total As and As(V) (**Figs. 8g-h**) demonstrated distinct patterns of high and low concentrations. For F^-, the majority of drinking water sources with high concentrations dominated the northeast section mainly in the lowlands underlie the migmatite-granitoid-meta-sediment complex. Some of the drinking water sources in this setting had F^- exceeding the recommended guideline value of 1.5 mg/L (WHO, 2017). The drinking water pH in this setting was also high indicating the alkaline environment favoring the mobilization of F^- in water through the water-rock interaction. The majority of the drinking water sources with low F^- concentrations dominated parts of the volcano-sedimentary complex (Greenstone Belt with BIF) and in the southern section characterized by relative highlands. The pH in this section is also relatively low signifying that complexation of F^- with other metals may be taking place resulting in the reduction of the aqueous concentration of F^- ions.

The total As measured in situ (**Fig. 8g**) and As(V) measured in the laboratory (**Fig. 8h**) showed two distinct patterns with high and low As concentrations. Both high and low spatial patterns in As concentrations dominated the same locations to similar extents. All drinking water sources in the high spatial pattern category had values exceeding 10 µg/L, the maximum permissible limit of WHO. These drinking water sources with poor quality dominated the northeast and south of the study area. The drinking water sources with high levels of As in the northeast were also characterized by high levels of F^- signifying the co-occurrence of these elements in groundwater in these settings. The drinking water sources with high As occur predominantly in the southern part of the study area under intensive small-scale gold mining activities as well artisanal gold processing. The pH in this setting is low signifying the oxidizing environment. The high levels of As in this section is a result of oxidation of the arsenopyrite exposed to the surface through small-scale mining operations. As and F^-

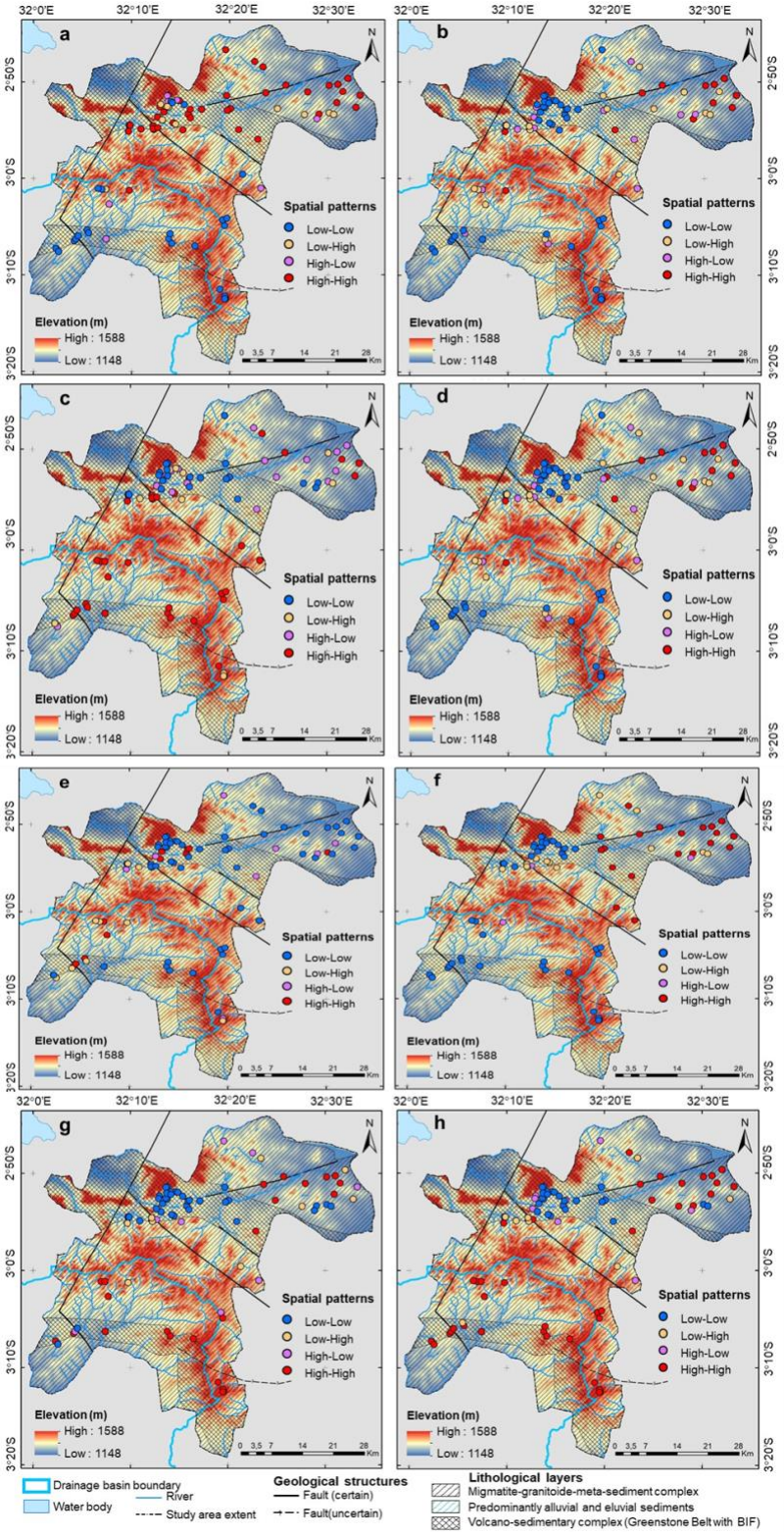

Figure 8. *Spatial distribution patterns of the water quality parameters in the Geita region. a) pH; b) EC; c) Eh; d) TDS; e) K+; f) F^-; g) Total As (measured in the field); and h) As(V) (analyzed in the laboratory).*

demonstrated spatial co-occurrence indicating possible environmental health risks including human beings due to prolonged consumption of elevated concentrations of such toxic elements through drinking water from contaminated groundwater sources (Kapaj et al., 2006; Litter et al., 2019). The co-occurrence of As and F^- dominated the northeast

section of the study area. The environment hosting these drinking water sources is reducing in nature as envisaged by the high pH values.

The spatial clustering and co-occurrence patterns of As and F^- (**Fig. 8**) reflect coupled effects of lithological variations, weathering intensity, and groundwater flow paths within the near surface weathering system. Elevated As concentrations in mining influenced zones are linked to oxidative weathering of sulfide bearing rocks, exposed during artisanal and small-scale gold mining, producing secondary Fe(III) oxides and hydroxides. Subsequent reductive dissolution under locally reducing conditions released the sorbed As from the surface of Fe-phases into groundwater, consistent with observed pH values and Ca-HCO_3 water types, explaining the elevated and spatially persistent concentrations of As. In parallel, F^- enrichment occurred primarily in alkaline Na–HCO_3 waters characterized by low Ca^{2+} activity, elevated Na^+ and HCO_3^- concentrations and active ion exchange, consistent with modeled undersaturation of fluorite and limited calcium availability due to calcite precipitation. Variations in groundwater residence time and fracture focused recharge further influenced geochemical reaction and mineral transformation, providing a mechanistic understanding of the observed Moran's I clusters and lithology linked hot spots. These results demonstrate that groundwater quality in the study area is governed by interacting weathering, transport, and redox processes operated within the Critical Zone rather than by isolated geochemical reactions (Brantley et al., 2006; Chorover et al., 2007; Brooks et al., 2015).

The observed co-occurrence of As and F^- reflects two complementary Critical Zone pathways. First, oxidative weathering of sulfide-bearing minerals and exposed artisanal and small-scale gold mining materials producing secondary Fe(III) oxides/hydroxides that subsequently undergo reductive dissolution, releasing adsorbed or co-precipitated As into groundwater. Second, alkaline Na–HCO_3 waters with low Ca^{2+} activity enhance F^- desorption, maintaining elevated dissolved F^- along longer, and more alkaline flow paths. Together, these Critical Zone mediated feedback explain the spatial clustering and the alignment of high As and F^- zones with specific hydrostratigraphic domains.

5 Conclusion

This study demonstrates that groundwater in the Geita district is affected by the geogenic co-occurrence of As and F^-, with most As concentrations and a smaller fraction of F^- concentrations exceeding the WHO's guideline values. Spatial clustering and co-occurrence show clear associations with lithological domains and zones influenced by artisanal and small-scale gold mining. Interpreted within a Critical Zone perspective, these patterns arise from interaction among geological settings, weathering profiles, and groundwater flow paths that collectively regulate mineral surface reactivity and pH and redox conditions of the aquifers. Oxidative weathering of sulfide-bearing rocks forms Fe oxides and hydroxides that can subsequently undergo reductive dissolution, releasing As into groundwater. In contrast, alkaline Na–HCO_3 waters with low Ca^{2+} activity promote ion exchange and calcite precipitation, which can reduce availability of Ca^{2+} and limit precipitation of fluorite thereby maintaining F^- in the aqueous phase. These coupled processes provide a mechanistic explanation for the observed spatial heterogeneity and explain the co-occurrence As and F^- in Precambrian basement aquifers of the Lake Victoria Basin. Understanding patterns of groundwater quality evolution through Critical Zone processes therefore supports risk assessment and the design of targeted mitigation strategies that focus on specific hydrostratigraphic domains, with priority given to zones affected by mining, alkaline Na–HCO_3 waters with low calcium activity, and areas that show strong spatial clustering of As and F^-. Future work should extend the analysis to include seasonal variability and examine both geogenic and anthropogenic sources to enhance the prediction and management of groundwater quality in the region.

6 Data availability statement

The data can be found in the supplementary information. Additional data can be made available upon request.

7 Ethical statements

Ethical approval was not required for this study.

8 Conflict of interest

The authors declare that they have no known competing financial interests or personal relationships that could have appeared to influence the work reported in this paper.

9 Acknowledgement

We sincerely thank Swedish International Development Cooperation Agency (Sida) for funding this study which was carried out under the framework of bilateral collaboration between KTH Royal Institute of Technology and the University of Dar es Salaam through the DAFWAT project, (Project Number 2235, Sida contribution number

51170071). We also thank the Ministry of Water in Tanzania through regional and water basin offices for providing the necessary logistics during the water sampling campaign.

10 Author contributions

F. Ligate: Conceptualization, data curation, methodology, writing – original draft, and writing – review & editing. J. Ijumulana: Visualization, and writing – review & editing. R. Irunde: Writing – review & editing. V. Kimambo: Writing – review & editing. R. Hamisi: Writing – review & editing. J.P. Maity: Writing – review & editing. J. Mtamba: Funding acquisition, project administration, and writing – review & editing. F. Mtalo: Funding acquisition, project administration, supervision, and writing – review & editing. P. Bhattacharya: Funding acquisition, project administration, supervision, and writing – review & editing. All authors approved the final version of the manuscript.

11 Copyright statement

This is an open access article distributed under the terms and conditions of the Creative Commons Attribution (CC BY NC ND) license (https://creativecommons.org/licenses/by-nc-nd/4.0/). © 2026 by the authors. Licensee Enviro Mind Solutions, Connecticut, USA.

References

Addison, M. J., Rivett, M. O., Robinson, H., Fraser, A., Miller, A. M., Phiri, P., Mleta, P., & Kalin, R. M. (2020). Fluoride occurrence in the lower East African Rift System, Southern Malawi. Science of The Total Environment, 712, 136260. https://doi.org/10.1016/j.scitotenv.2019.136260

Ahmed, K. M., Bhattacharya, P., Hasan, M. A., Akhter, S. H., Alam, S. M. M., Bhuyian, M. A. H., Imam, M. B., Khan, A. A., & Sracek, O. (2004). Arsenic enrichment in groundwater of the alluvial aquifers in Bangladesh: an overview. Applied Geochemistry, 19(2), 181–200. https://doi.org/10.1016/j.apgeochem.2003.09.006

Alarcón-Herrera, M. T., Martin-Alarcon, D. A., Gutiérrez, M., Reynoso-Cuevas, L., Martín-Domínguez, A., Olmos-Márquez, M. A., & Bundschuh, J. (2020). Co-occurrence, possible origin, and health-risk assessment of arsenic and fluoride in drinking water sources in Mexico: Geographical data visualization. Science of The Total Environment, 698, 134168. https://doi.org/10.1016/j.scitotenv.2019.134168

Almås, Å. R., & Manoko, M. L. K. (2012). Trace element concentrations in soil, sediments, and waters in the vicinity of Geita Gold Mines and North Mara Gold Mines in Northwest Tanzania. Soil and Sediment Contamination: An International Journal, 21(2), 135–159. https://doi.org/10.1080/15320383.2012.649372

Anderson, S. P., von Blanckenburg, F., & White, A. F. (2007). Physical and chemical controls on the Critical Zone. Elements, 3(5), 315–319. https://doi.org/10.2113/gselements.3.5.315

Aullón Alcaine, A., Schulz, C., Bundschuh, J., Jacks, G., Thunvik, R., Gustafsson, J.-P., Mörth, C.-M., Sracek, O., Ahmad, A., & Bhattacharya, P. (2020). Hydrogeochemical controls on the mobility of arsenic, fluoride and other geogenic co-contaminants in the shallow aquifers of northeastern La Pampa Province in Argentina. Science of The Total Environment, 715, 136671. https://doi.org/10.1016/j.scitotenv.2020.136671

Bakyayita, G. K., Norrström, A. C., & Kulabako, R. N. (2019). Assessment of levels, speciation, and toxicity of trace metal contaminants in selected shallow groundwater sources, surface runoff, wastewater, and surface water from designated streams in Lake Victoria Basin, Uganda. Journal of Environmental and Public Health, 2019, 1–18. https://doi.org/10.1155/2019/6734017

Bhattacharya, P., & Bundschuh, J. (2015). Groundwater for sustainable development – cross cutting the UN sustainable development goals – editorial. Groundwater for Sustainable Development, 1(1–2), 155–157. https://doi.org/10.1016/j.gsd.2016.04.004

Bhattacharya, P., Chatterjee, D., & Jacks, G. (1997). Occurrence of arsenic-contaminated groundwater in alluvial aquifers from delta plains, Eastern India: Options for safe drinking water supply. International Journal of Water Resources Development, 13(1), 79–92. https://doi.org/10.1080/07900629749944

Brantley, S., White, T.S., White, A.F., Sparks, D., Richter, D., Pregitzer, K., Derry, L., Chorover, J., Chadwick, O., April, R., Anderson, S., Amundson, R., (2006): Frontiers in Exploration of the Critical Zone: Report of a workshop sponsored by the National Science Foundation (NSF), October 24-26, 2005. Newark, DE, 30 pp.

BGS (2019, September 30). Africa Groundwater Atlas. https://www.bgs.ac.uk/geology-projects/africa-groundwater-atlas/

Brooks, P. D., Chorover, J., Fan, Y., Godsey, S. E., Maxwell, R. M., McNamara, J. P., & Tague, C. (2015). Hydrological partitioning in the critical zone: Recent advances and opportunities for developing transferable understanding of water cycle dynamics. Water

Resources Research, 51(9), 6973–6987. https://doi.org/10.1002/2015wr017039

Brunt, R., Vasak, L., & Groffioen, J. (2004). Fluoride in groundwater: Probablity of occurrence of excessive concentration on global scale (SP 2004-2).

Bundschuh, J., Maity, J. P., Mushtaq, S., Vithanage, M., Seneweera, S., Schneider, J., Bhattacharya, P., Khan, N. I., Hamawand, I., Guilherme, L. R. G., Reardon-Smith, K., Parvez, F., Morales-Simfors, N., Ghaze, S., Pudmenzky, C., Kouadio, L., & Chen, C.-Y. (2017). Medical geology in the framework of the sustainable development goals. Science of The Total Environment, 581–582, 87–104. https://doi.org/10.1016/j.scitotenv.2016.11.208

Bundschuh, J., Schneider, J., Alam, M. A., Niazi, N. K., Herath, I., Parvez, F., Tomaszewska, B., Guilherme, L. R. G., Maity, J. P., López, D. L., Cirelli, A. F., Pérez-Carrera, A., Morales-Simfors, N., Alarcón-Herrera, M. T., Baisch, P., Mohan, D., & Mukherjee, A. (2021). Seven potential sources of arsenic pollution in Latin America and their environmental and health impacts. Science of The Total Environment, 780, 146274. https://doi.org/10.1016/j.scitotenv.2021.146274

Centeno, J. A., Mullick, F. G., Martinez, L., Page, N. P., Gibb, H., Longfellow, D., Thompson, C., & Ladich, E. R. (2002). Pathology related to chronic arsenic exposure. Environmental Health Perspectives, 110(suppl 5), 883–886. https://doi.org/10.1289/ehp.02110s5883

Chandrajith, R., Diyabalanage, S., & Dissanayake, C. B. (2020). Geogenic fluoride and arsenic in groundwater of Sri Lanka and its implications to community health. Groundwater for Sustainable Development, 10, 100359. https://doi.org/10.1016/j.gsd.2020.100359

Chorover, J., Kretzschmar, R., Garcia-Pichel, F., & Sparks, D. L. (2007). Soil biogeochemical processes within the critical zone. Elements, 3(5), 321–326. https://doi.org/10.2113/gselements.3.5.321

Choudhury, R., Nath, B., Rahman, M. M., Medhi, S., & Dutta, J. (2024). Hydrogeochemical characteristics of groundwater contamination in Guwahati city, Assam, India: Tracing the elemental Threads. Journal of Environmental Management, 359, 120933. https://doi.org/10.1016/j.jenvman.2024.120933

Cook, Y. A., Sanislav, I. V., Hammerli, J., Blenkinsop, T. G., & Dirks, P. H. G. M. (2016). A primitive mantle source for the Neoarchean mafic rocks from the Tanzania Craton. Geoscience Frontiers, 7(6), 911–926. https://doi.org/10.1016/j.gsf.2015.11.008

De, A., Mridha, D., Joardar, M., Das, A., Chowdhury, N. R., & Roychowdhury, T. (2022). Distribution, prevalence and health risk assessment of fluoride and arsenic in groundwater from lower Gangetic plain in West Bengal, India. Groundwater for Sustainable Development, 16, 100722. https://doi.org/10.1016/j.gsd.2021.100722

Dissanayake, C. B. (1991). The fluoride problem in the ground water of Sri Lanka — environmental management and health. International Journal of Environmental Studies, 38(2–3), 137–155. https://doi.org/10.1080/00207239108710658

EPA, U. S. (2007). US EPA Method 200.8: Determination of Trace Elements in Waters and Wastes by Inductively Coupled Plasma Optical Emission Spectrometry (ICP-OES). In.

EPA, U. S. (2017). Groundwater sampling (SESDPROC301-R4).

FDMT. (2016). Flood & drought management tools. Retrieved from http://fdmt.iwlearn.org/en

Fernandes, R. M. S., Miranda, J. M., Delvaux, D., Stamps, D. S., & Saria, E. (2013). Re-evaluation of the kinematics of Victoria Block using continuous GNSS data. Geophysical Journal International, 193(1), 1–10. https://doi.org/10.1093/gji/ggs071

Gayathri, J. A., Raj, V. T., Sreelash, K., Maya, K., & Padmalal, D. (2026). Tracing the causes of fluoride enrichment in the groundwater sources of the Upper Bhavani River Basin, Southwest India–An integrated approach for its management in mountainous terrains. Groundwater for Sustainable Development, 32, 101557. https://doi.org/10.1016/j.gsd.2025.101557

Ghiglieri, G., Balia, R., Oggiano, G., & Pittalis, D. (2010). Prospecting for safe (low fluoride) groundwater in the Eastern African Rift: the Arumeru District (Northern Tanzania). Hydrology and Earth System Sciences, 14(6), 1081–1091. https://doi.org/10.5194/hess-14-1081-2010

González-Horta, C., Ballinas-Casarrubias, L., Sánchez-Ramírez, B., Ishida, M., Barrera-Hernández, A., Gutiérrez-Torres, D., Zacarias, O., Saunders, R., Drobná, Z., Mendez, M., García-Vargas, G., Loomis, D., Stýblo, M., & Del Razo, L. (2015). A concurrent exposure to arsenic and fluoride from drinking water in Chihuahua, Mexico. International Journal of Environmental Research and Public Health, 12(5), 4587–4601. https://doi.org/10.3390/ijerph120504587

Gustafsson, J. P. (2022). Visual MINTEQ Program Version 3.1. Retrieved December 2022 from http://vminteq.com

Henckel, J., Poulsen, K. H., Sharp, T., & Spora, P. (2016). Lake Victoria Goldfields. Episodes, 39(2), 135–154. https://doi.org/10.18814/epiiugs/2016/v39i2/95772

Ijumulana, J., Lucca, E., Bhattacharya, P., & Mtalo, F. (2017). Mineral solubility controls on drinking water quality in

the areas of gold mining in geita and Mara regions of northern Tanzania. GSA Annual Meeting, Seattle, Washington, USA.

Ijumulana, J., Ligate, F., Bhattacharya, P., Mtalo, F., & Zhang, C. (2020). Spatial analysis and GIS mapping of regional hotspots and potential health risk of fluoride concentrations in groundwater of northern Tanzania. Science of The Total Environment, 735, 139584. https://doi.org/10.1016/j.scitotenv.2020.139584

Ijumulana, J., Ligate, F., Irunde, R., Bhattacharya, P., Ahmad, A., Tomašek, I., Maity, J. P., & Mtalo, F. (2022). Spatial variability of the sources and distribution of fluoride in groundwater of the Sanya alluvial plain aquifers in northern Tanzania. Science of The Total Environment, 810, 152153. https://doi.org/10.1016/j.scitotenv.2021.152153

Ikingura, J. R., Akagi, H., Mujumba, J., & Messo, C. (2006). Environmental assessment of mercury dispersion, transformation and bioavailability in the Lake Victoria Goldfields, Tanzania. Journal of Environmental Management, 81(2), 167–173. https://doi.org/10.1016/j.jenvman.2005.09.026

Irunde, R., Ijumulana, J., Ligate, F., Maity, J. P., Ahmad, A., Mtamba, J., Mtalo, F., & Bhattacharya, P. (2022). Arsenic in Africa: potential sources, spatial variability, and the state of the art for arsenic removal using locally available materials. Groundwater for Sustainable Development, 18, 100746. https://doi.org/10.1016/j.gsd.2022.100746

Jacks, G., Bhattacharya, P., & Harikumar, P. S. (2005, August 21-27, 2005). Irrigated agriculture and the formation of high fluoride groundwaters in India. Volume, The 15th Stockholm Water Symposium, Drainage Basin Management- Hard and Soft Solutions in Regional Development, Stockholm.

Jacks, G., & Nystrand, M. (2019). Speciation of trace elements in groundwater, surface water and sediments: a short review. Environmental Earth Sciences, 78(12). https://doi.org/10.1007/s12665-019-8334-9

Kapaj, S., Peterson, H., Liber, K., & Bhattacharya, P. (2006). Human health effects from chronic arsenic poisoning--a review. Journal of Environmental Science and Health, Part A, 41(10), 2399–2428. https://doi.org/10.1080/10934520600873571

Kaseva, M. E., Mayige, C., Salukele, F., Mkongo, G., & Sangeti, E. M. (2018). Spatial Distribution of Fluoride Concentration in Drinking Water Sources in Northern Tanzania. Journal of Civil and Environmental Research, 10, 41-51.

Kassenga, G., & Mato, R. (2008). Arsenic contamination levels in drinking water sources in mining areas in Lake Victoria Basin, Tanzania, and its removal using stabilized ferralsols. International Journal of Biological and Chemical Sciences, 2(4), 389-400. http://www.ajol.info

Kimambo, V., Bhattacharya, P., Mtalo, F., Mtamba, J., & Ahmad, A. (2019). Fluoride occurrence in groundwater systems at global scale and status of defluoridation – State of the art. Groundwater for Sustainable Development, 9, 100223. https://doi.org/10.1016/j.gsd.2019.100223

Kumar, M., Das, N., Goswami, R., Sarma, K. P., Bhattacharya, P., & Ramanathan, AL. (2016). Coupling fractionation and batch desorption to understand arsenic and fluoride co-contamination in the aquifer system. Chemosphere, 164, 657–667. https://doi.org/10.1016/j.chemosphere.2016.08.075

Kumar, S., Singh, R., Venkatesh, A. S., Udayabhanu, G., & Sahoo, P. R. (2019). Medical Geological assessment of fluoride contaminated groundwater in parts of Indo-Gangetic Alluvial plains. Scientific Reports, 9(1), 16243. https://doi.org/10.1038/s41598-019-52812-3

Kumar, R., Ali, S., Sandanayake, S., Islam, Md. A., Ijumulana, J., Maity, J. P., Vithanage, M., Armienta, M. A., Sharma, P., Hamisi, R., Kimambo, V., & Bhattacharya, P. (2024). Fluoride as a global groundwater contaminant. In Inorganic Contaminants and Radionuclides (pp. 319–350). Elsevier. https://doi.org/10.1016/b978-0-323-90400-1.00010-0

Ligate, F., Ijumulana, J., Ahmad, A., Kimambo, V., Irunde, R., Mtamba, J. O., Mtalo, F., & Bhattacharya, P. (2021). Groundwater resources in the East African Rift Valley: Understanding the geogenic contamination and water quality challenges in Tanzania. Scientific African, 13, e00831. https://doi.org/10.1016/j.sciaf.2021.e00831

Ligate, F., Lucca, E., Ijumulana, J., Irunde, R., Kimambo, V., Mtamba, J., Ahmad, A., Hamisi, R., Maity, J. P., Mtalo, F., & Bhattacharya, P. (2022). Geogenic contaminants and groundwater quality around Lake Victoria goldfields in northwestern Tanzania. Chemosphere, 307, 135732. https://doi.org/10.1016/j.chemosphere.2022.135732

Litter, M. I., Ingallinella, A. M., Olmos, V., Savio, M., Difeo, G., Botto, L., Torres, E. M. F., Taylor, S., Frangie, S., Herkovits, J., Schalamuk, I., González, M. J., Berardozzi, E., García Einschlag, F. S., Bhattacharya, P., & Ahmad, A. (2019). Arsenic in Argentina: Technologies for arsenic removal from groundwater sources, investment costs and waste management practices. Science of The Total Environment, 690, 778–789. https://doi.org/10.1016/j.scitotenv.2019.06.358

Lucca, E. (2017). Geochemical Investigation of Arsenic in Drinking Water Sources in Proximity of Gold Mining

Areas within the Lake Victoria Basin, in Northern Tanzania [MSc, KTH Royal Institute of Technology]. Stockholm, Sweden.

MacDonald, A. M., Bonsor, H. C., Dochartaigh, B. É. Ó., & Taylor, R. G. (2012). Quantitative maps of groundwater resources in Africa. Environmental Research Letters, 7(2), 024009. https://doi.org/10.1088/1748-9326/7/2/024009

Maher, K. (2010). The dependence of chemical weathering rates on fluid residence time. Earth and Planetary Science Letters, 294(1–2), 101–110. https://doi.org/10.1016/j.epsl.2010.03.010

Maity, J. P., Nath, B., Kar, S., Chen, C.-Y., Banerjee, S., Jean, J.-S., Liu, M.-Y., Centeno, J. A., Bhattacharya, P., Chang, C. L., & Santra, S. C. (2012). Arsenic-induced health crisis in peri-urban Moyna and Ardebok villages, West Bengal, India: an exposure assessment study. Environmental Geochemistry and Health, 34(5), 563–574. https://doi.org/10.1007/s10653-012-9458-y

Marinović Ruždjak, A., & Ruždjak, D. (2015). Evaluation of river water quality variations using multivariate statistical techniques. Environmental Monitoring and Assessment, 187(4). https://doi.org/10.1007/s10661-015-4393-x

Mbabaye, G. K., Minja, R. J., Mtalo, F. W., Legonda, I., & Mkongo, G. (2018). Flouride occurence in domestic water supply sources in Tanzania: A case of Arumeru District Arusha Region. Tanzania Journal of Science, 44(3), 72-92.

Mosha, D. B., Gudaga, J. L., Gama, D., & J, K. J. (2022). Valuing groundwater use: Resolving the potential of groundwater in the Upper Great Ruaha River Catchment of Tanzania. In V. Re, R. L. Manzione, T. A. Abiye, A. Mukherji, & A. MacDonald (Eds.), *Groundwater for Sustainable Livelihoods and Equitable Growth* (1st ed., pp. 392). CRC Press. https://doi.org/10.1201/9781003024101

Mridha, D., Priyadarshni, P., Bhaskar, K., Gaurav, A., De, A., Das, A., Joardar, M., Chowdhury, N. R., & Roychowdhury, T. (2021). Fluoride exposure and its potential health risk assessment in drinking water and staple food in the population from fluoride endemic regions of Bihar, India. Groundwater for Sustainable Development, 13, 100558. https://doi.org/10.1016/j.gsd.2021.100558

Nyanza, E. C., Bernier, F. P., Manyama, M., Hatfield, J., Martin, J. W., & Dewey, D. (2019). Maternal exposure to arsenic and mercury in small-scale gold mining areas of Northern Tanzania. Environmental Research, 173, 432–442. https://doi.org/10.1016/j.envres.2019.03.031

Patel, K. S., Sahu, B. L., Dahariya, N. S., Bhatia, A., Patel, R. K., Matini, L., Sracek, O., & Bhattacharya, P. (2015). Groundwater arsenic and fluoride in Rajnandgaon District, Chhattisgarh, northeastern India. Applied Water Science, 7(4), 1817–1826. https://doi.org/10.1007/s13201-015-0355-2

Podgorski, J., & Berg, M. (2020). Global threat of arsenic in groundwater. Science, 368(6493), 845–850. https://doi.org/10.1126/science.aba1510

Quino Lima, I., Ramos Ramos, O., Ormachea Muñoz, M., Quintanilla Aguirre, J., Duwig, C., Maity, J. P., Sracek, O., & Bhattacharya, P. (2020). Spatial dependency of arsenic, antimony, boron and other trace elements in the shallow groundwater systems of the Lower Katari Basin, Bolivian Altiplano. Science of The Total Environment, 719, 137505. https://doi.org/10.1016/j.scitotenv.2020.137505

Rafique, T., Naseem, S., Usmani, T. H., Bashir, E., Khan, F. A., & Bhanger, M. I. (2009). Geochemical factors controlling the occurrence of high fluoride groundwater in the Nagar Parkar area, Sindh, Pakistan. Journal of Hazardous Materials, 171(1–3), 424–430. https://doi.org/10.1016/j.jhazmat.2009.06.018

Rahman, M. M., Mukherjee, D., Sengupta, M. K., Chowdhury, U. K., Lodh, D., Chanda, C. R., Roy, S., Selim, Md., Quamruzzaman, Q., Milton, A. H., Shahidullah, S. M., Rahman, Md. T., & Chakraborti, D. (2002). Effectiveness and reliability of arsenic field testing kits: Are the million dollar screening projects effective or not? Environmental Science & Technology, 36(24), 5385–5394. https://doi.org/10.1021/es020591o

Ramos Ramos, O. E., Tapia, M. I. C., Lima, I. Q., Rötting, T. S., Orsag, V., Chambi, L., Sracek, O., Aguirre, J. Q., Maity, J. P., Ahmad, A., Bundschuh, J., & Bhattacharya, P. (2025). Trace elements in soils and their uptake by crops: Insights from a legacy mining area in Oruro, Bolivian Altiplano. Journal of Environmental Science, Health & Sustainability, 1(1), 8–26. https://doi.org/10.63697/jeshs.2025.029

Rango, T., Kravchenko, J., Atlaw, B., McCornick, P. G., Jeuland, M., Merola, B., & Vengosh, A. (2012). Groundwater quality and its health impact: An assessment of dental fluorosis in rural inhabitants of the Main Ethiopian Rift. Environment International, 43, 37–47. https://doi.org/10.1016/j.envint.2012.03.002

Rango, T., Vengosh, A., Dwyer, G., & Bianchini, G. (2013). Mobilization of arsenic and other naturally occurring contaminants in groundwater of the Main Ethiopian Rift aquifers. Water Research, 47(15), 5801–5818. https://doi.org/10.1016/j.watres.2013.07.002

Reid, M. S., Hoy, K. S., Schofield, J. R. M., Uppal, J. S., Lin, Y., Lu, X., Peng, H., & Le, X. C. (2020). Arsenic speciation analysis: A review with an emphasis on chromatographic separations. TrAC Trends in Analytical Chemistry, 123, 115770. https://doi.org/10.1016/j.trac.2019.115770

Rezaei, M., Nikbakht, M., & Shakeri, A. (2017). Geochemistry and sources of fluoride and nitrate contamination of groundwater in Lar area, south Iran. Environmental Science and Pollution Research, 24(18), 15471–15487. https://doi.org/10.1007/s11356-017-9108-0

Singh, C. K., Rina, K., Singh, R. P., Shashtri, S., Kamal, V., & Mukherjee, S. (2011). Geochemical modeling of high fluoride concentration in groundwater of Pokhran area of Rajasthan, India. Bulletin of Environmental Contamination and Toxicology, 86(2), 152–158. https://doi.org/10.1007/s00128-011-0192-4

Stolze, L., Battistel, M., & Rolle, M. (2022). Oxidative dissolution of arsenic-bearing sulfide minerals in groundwater: Impact of hydrochemical and hydrodynamic conditions on arsenic release and surface evolution. Environmental Science & Technology, 56(8), 5049–5061. https://doi.org/10.1021/acs.est.2c00309

Sunkari, E. D., Adams, S. J., Okyere, M. B., & Bhattacharya, P. (2022). Groundwater fluoride contamination in Ghana and the associated human health risks: Any sustainable mitigation measures to curtail the long term hazards? Groundwater for Sustainable Development, 16, 100715. https://doi.org/10.1016/j.gsd.2021.100715

TGS (2018, December, 15). Tanzania Geological Society. https://www.tgs.or.tz/

Thole, B. (2013). Ground water contamination with fluoride and potential fluoride removal technologies for east and Southern Africa. In Perspectives in Water Pollution. InTech. https://doi.org/10.5772/54985

Tibebe, D., Zewge, F., Lemma, B., & Kassa, Y. (2022). Assessment of spatio-temporal variations of selected water quality parameters of Lake Ziway, Ethiopia using multivariate techniques. BMC Chemistry, 16(1). https://doi.org/10.1186/s13065-022-00806-0

Tomašek, I., Mouri, H., Dille, A., Bennett, G., Bhattacharya, P., Brion, N., Elskens, M., Fontijn, K., Gao, Y., Gevera, P. K., Ijumulana, J., Kisaka, M., Leermakers, M., Shemsanga, C., Walraevens, K., Wragg, J., & Kervyn, M. (2022). Naturally occurring potentially toxic elements in groundwater from the volcanic landscape around Mount Meru, Arusha, Tanzania and their potential health hazard. Science of The Total Environment, 807, 150487. https://doi.org/10.1016/j.scitotenv.2021.150487

UNEP. (2006). Lake Victoria Basin Environment Outlook: Environment and Development.

URT. (2013). 2012 Population and housing census. National Bureau of Statistics.

Vithanage, M., & Bhattacharya, P. (2015). Fluoride in the environment: sources, distribution and defluoridation. Environmental Chemistry Letters, 13(2), 131–147. https://doi.org/10.1007/s10311-015-0496-4

White, T., Brantley, S., Banwart, S., Chorover, J., Dietrich, W., Derry, L., Lohse, K., Anderson, S., Aufdendkampe, A., Bales, R., Kumar, P., Richter, D., & McDowell, B. (2015). The role of critical zone observatories in critical zone science. In Developments in Earth Surface Processes (pp. 15–78). Elsevier. https://doi.org/10.1016/b978-0-444-63369-9.00002-1

WHO. (2017). Guideline for drinking-water quality. World Health Organization.

Xing, S., Guo, H., Wu, P., Hu, X., Zhao, Z., & Yuan, Y. (2022). Distribution and formation processes of high fluoride groundwater in different types of aquifers in the Hualong-Xunhua Basin. Earth Science Frontiers, 29(3), 115–128. https://doi.org/10.13745/j.esf.sf.2022.1.34

Publisher's note

The author(s) are solely responsible for the opinions and data presented in this article, and publisher or the editor(s) disclaim responsibility for any injury to people or property caused by any ideas mentioned in this article.